SPINK3-sperm interaction determines a stable sperm subpopulation with intact CatSper channel

Anabella R. Nicolli[1]*, Xiaofang Huang[2]*, Lucia Zalazar[1], Cintia Stival[4], Lucila R. Gomez-Olivieri[5], Gianluca Demare[1], Ana Romarowski[5], Mariano G. Buffone[5], Dario Krapf[4], Jean-Ju Chung[2,3] and Andreina Cesari[1]

*Equal contribution

1- Instituto de Investigaciones Biológicas (IIB-FCEyN/CONICET), Facultad de Ciencias Exactas y Naturales, Universidad Nacional de Mar del Plata, Consejo Nacional de Investigaciones Científicas y Técnicas (CONICET), Mar del Plata, Argentina.
2- Department of Cellular & Molecular Physiology, Yale University School of Medicine, New Haven, CT 06510, USA
3- Department of Ob/Gyn & Reproductive Sciences, Yale University School of Medicine, New Haven, CT 06510, USA
4- Cell Signal Transduction Networks Laboratory, Instituto de Biología Molecular y Celular de Rosario (IBR, CONICET-UNR), Rosario, Argentina
5- Instituto de Biología y Medicina Experimental (IBYME-CONICET), Ciudad Autónoma de Buenos Aires, Argentina.

Corresponding author: Andreina Cesari; Funes 3250 3rd floor, Mar del Plata, Argentina; +5492235134227; andreinacesari@gmail.com

GRAPHICAL ABSTRACT

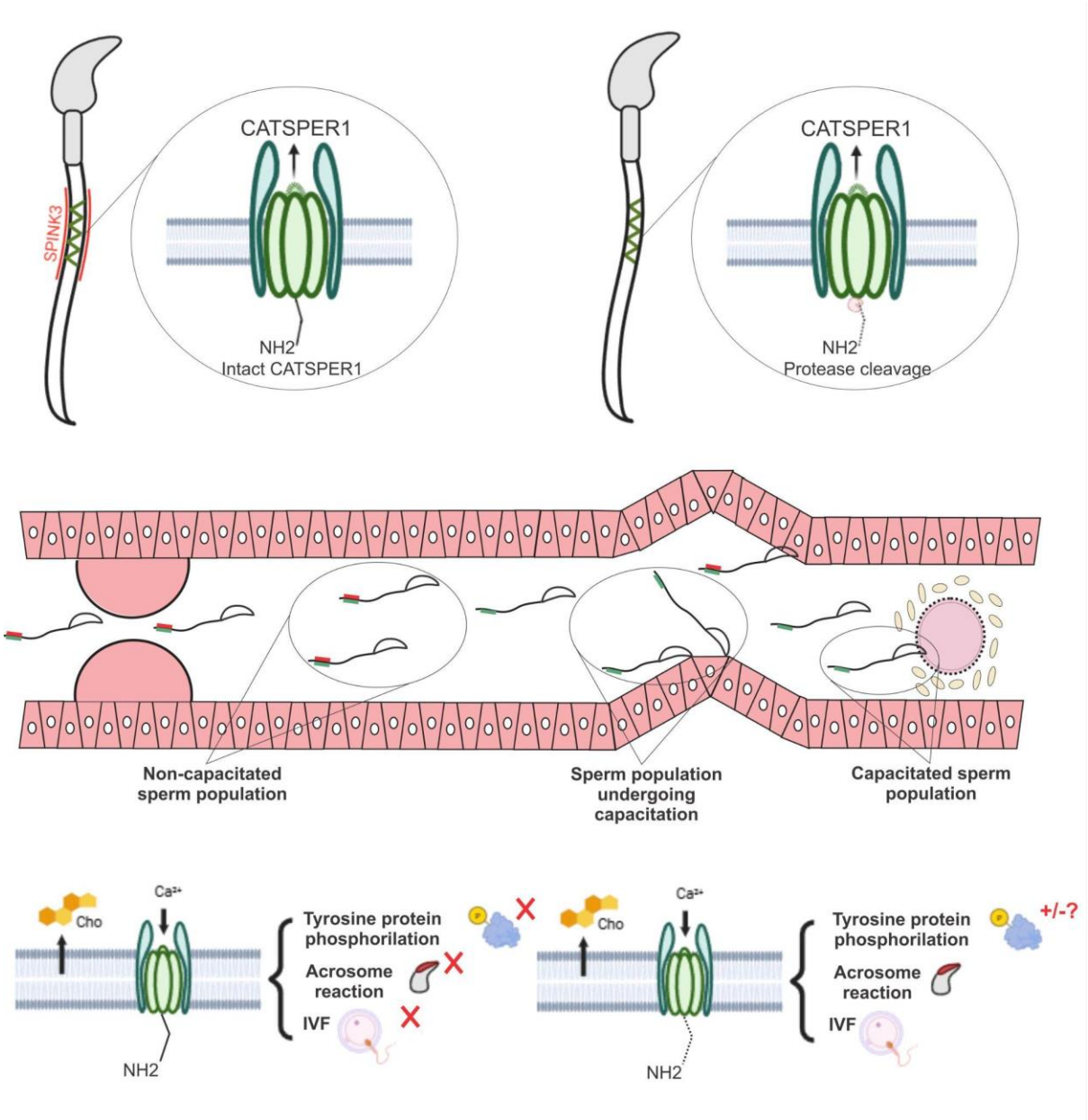

ABSTRACT

Sperm capacitation involves proteolytic remodeling of membrane proteins, including components of the CatSper calcium channel, which is essential for hyperactivation and male fertility. Here, we identify the seminal protease inhibitor SPINK3, a known decapacitation factor that suppresses premature capacitation in the female tract, as the first physiological inhibitor of CATSPER1 processing. In mouse sperm, SPINK3 blocks capacitation-induced CATSPER1 cleavage, preserving a subpopulation with intact CatSper channels and lacking pTyr development in the flagellum. SPINK3 localizes to the outer surface of the sperm principal piece membrane in a CatSper-dependent but non-quadrilateral pattern, stabilizes membrane

organization, and delays cholesterol efflux. These results reveal SPINK3 as a multifunctional regulator of capacitation, shaping sperm subpopulations in the female reproductive tract.

Keywords: sperm capacitation, SPINK3, CATSPER1, protease inhibition, membrane stabilization, decapacitation factors

SIGNIFICANCE STATEMENT

This study unveils a novel physiological regulator from the male reproductive tract, SPINK3, which extracellularly controls the processing of CATSPER1, a key subunit of the CatSper calcium channel essential for sperm capacitation in mice. We show that SPINK3 binds to the sperm surface and prevents the processing of CATSPER1 during capacitation. SPINK3-sperm interaction is dependent on the presence of the sperm-specific CatSper channel. Our findings reveal that SPINK3 stabilizes sperm membranes providing new insights into the molecular regulation of sperm function and fertility.

INTRODUCTION

The sperm journey begins in the male reproductive tract, where millions of sperm undergo surface modifications induced by male secretory molecules (1). After ejaculation, mammalian sperm must undergo biochemical and functional changes within the female reproductive tract, a process collectively known as capacitation (2, 3). This process involves membrane remodeling and the activation of intracellular signaling pathways leading to the acquisition of fertilizing ability. Decapacitation factors, typically originating from the male reproductive tract or seminal plasma, coat and stabilize the sperm surface after ejaculation, preventing or delaying capacitation until the sperm reaches an appropriate environment in the female reproductive tract (1, 4, 5).

CatSper is the primary Ca^{2+} channel in mammalian spermatozoa, consisting of four pore-forming subunits (CATSPER1, 2, 3, 4) and at least ten additional auxiliary subunits (6). This channel is specifically located in the flagellar membrane of the principal piece, exhibiting pH sensitivity and weak voltage dependence (7, 8) and is essential for the development of hyperactivated motility of sperm (9, 10). Infertility has been observed in male mice lacking the *Catsper* genes encoding the transmembrane subunits (7, 9–13). Capacitation induces specific cleavage and processing of CATSPER1, one of the pore-forming subunits, in the cytosolic N-terminus by unknown sperm enzyme(s), resulting in a graded distribution of heterogeneous sperm populations with varying degrees of CATSPER1 integrity along the female reproductive tract (14, 15). Spermatozoa that reach the ampulla, where fertilization takes place, mostly have intact CATSPER1 signal compared to those that remain behind the utero-tubal junction (UTJ). Recently, it was reported that another CatSper transmembrane subunit, CATSPERθ, which is essential for the CatSper channel assembly and serves as a checkpoint for flagellar trafficking during spermiogenesis, is also processed during sperm capacitation (12). This highlights the proteolytic regulation of the CatSper channels as a sperm selection mechanism. Although the cell-permeable potent proteasome inhibitor MG-132, as well as calpain inhibitors and the phosphatase 1/2A inhibitor calyculin A, have been shown to inhibit CATSPER1 processing (14, 15), physiological inhibitors responsible for modulating the processing of CatSper subunits remains unidentified.

SPINK3 (also known as P12 or SPINK1) is a small and highly conserved protein consisting of 80 amino acids, naturally secreted by the male seminal vesicles of most

114 mammals (16–18). It contains a Kazal domain that acts as a substrate analogue by
115 competitively and stoichiometrically binding to the active site of its target protease, forming a
116 stable protease–protease inhibitor complex, such as kallikreins, trypsin and chymotrypsin-like
117 proteases (19). SPINK3 also has a sperm binding domain (20) and attaches to sperm during
118 ejaculation (21). SPINK3 is a known decapacitation factor regulating SRC tyrosine kinase
119 activation and membrane potential, apparently without affecting the tyrosine kinase or PKA
120 activity. (18). The BSA-induced increase in intracellular Ca^{2+} concentration ($[Ca^{2+}]_i$) was
121 demonstrated to depend on CatSper channels. This $[Ca^{2+}]_i$ increase and CatSper activity are
122 inhibited by the presence of SPINK3 (18), suggesting an either direct or indirect blockade of
123 calcium entry through the CatSper channel. Similar to other decapacitation factors (22–24),
124 SPINK3 has been demonstrated to bind sperm during ejaculation until detachment in the
125 female tract, following a specific but asynchronous spatiotemporal kinetics, and contributing
126 to sperm heterogeneity (21). The protease TESP1 is the only natural target reported for
127 SPINK3 on the sperm head and this interaction was found to be blocked by the soybean
128 trypsin inhibitor, SBTI (25).
129 In this study, we show that SPINK3 regulates CATSPER1 processing and contributes
130 to the generation of sperm subpopulations with different capacitation states. This action is
131 accompanied by the stabilization of the sperm plasma membrane, suggesting that its
132 regulatory effect may involve protease inhibition and membrane-stabilizing mechanisms that
133 prevent protease access to CATSPER1 cleavage sites. These findings highlight a multifaceted
134 role for SPINK3 in modulating sperm capacitation.

135 **RESULTS**

136 **SPINK3 inhibits CATSPER1 processing induced by *in vitro* capacitation**
137
138 It has previously been reported that the cytoplasmic N-terminal domain of the
139 CATSPER1 undergoes proteolytic processing in sperm cells during capacitation, and the
140 progression of this processing is negatively correlated with the appearance of tyrosine
141 phosphorylation at single cell level *in vitro* and *in situ* (15). More recently, another CatSper
142 subunit, CATSPERθ, which plays a role in CatSper channel assembly and serves as a
143 checkpoint for CatSper flagellar trafficking, was also found to undergo capacitation-induced
144 degradation (12).
145 SPINK3 has previously been shown to inhibit CatSper channel activity (18). As this
146 small protein is not only a decapacitation factor but also a protease inhibitor, we hypothesize
147 that SPINK3 might be related to the regulation of CATSPER1 and/or CATSPERθ processing.
148 To test this idea, we evaluated capacitation-induced CATSPER1 and CATSPERθ protein
149 degradation in mouse sperm incubated under capacitating conditions, with or without SPINK3.
150 Interestingly, we found that the presence of SPINK3 abolished the degradation of CATSPER1,
151 but not CATSPERθ (**Figure 1A**). Consistent results were seen with anti-CATSPER1
152 immunostaining in mouse spermatozoa (**Figure 1B, Supp. Figure 1**). As sperm contains
153 several proteases (26), we assessed the proteolytic activity of sperm lysates using synthetic
154 substrates specific for trypsin, chymotrypsin, and elastase, in order to identify the protease
155 family targeted by SPINK3. Our results confirmed that trypsin-like activity was predominant,
156 and that this activity was inhibited by SPINK3, by seminal vesicle lysates (which contain native
157 SPINK3), and by commercial inhibitors such as PMSF (phenylmethylsulfonyl fluoride) and
158 SBTI (soybean trypsin inhibitor) (Figure 1C). As a control, we capacitated mouse spermatozoa

159 in the presence of SBTI and observed the same blocking effect on CATSPER1 processing
160 (**Supp. Figure 2**). Heterologously expressed full-length recombinant CATSPER1 has also
161 been validated for processing by sperm lysate *in vitro* due to the presence of specific
162 endogenous protease(s) (15). Similarly, this *in vitro* CATSPER1 processing was also inhibited
163 by the presence of SPINK3 (**Figure 1D**). Taken together, these results show that SPINK3
164 interferes with proteolytic processing of CATSPER1, by inhibiting sperm trypsin-like
165 protease(s). Furthermore, when sperm were preincubated with recombinant SPINK3 under
166 capacitating conditions, only spermatozoa lacking SPINK3 showed protein tyrosine
167 phosphorylation (pTyr) development in the flagella (**Figure 1E**), consistent with the previously
168 reported inverse correlation of pTyr and CatSper channel integrity (6, 14, 15). These results
169 support the idea that SPINK3 binding results in a population of sperm with intact CATSPER1
170 and SPINK3 bound to the flagellar surface.
171
172 **SPINK3 binds to the sperm flagellar membrane in a CatSper-dependent manner**
173
174 The CatSper channel forms four linear nanodomains along the flagellar membrane in
175 which the lipid raft marker caveolin1 resides (14). Recombinant SPINK3 can bind to raft
176 membrane domains in both acrosomal and tail membranes of non-capacitated mature
177 epididymal spermatozoa and this union is avoided by choleratoxin B supporting binding to
178 GM1 (18, 21). Given that SPINK3 is a secretory protein, we tested whether SPINK3 and
179 CatSper co-localize in the quadrilinear nanodomains. Confocal microscopy shows that, unlike
180 CATSPER1, which is localized exclusively to the principal piece, SPINK3 is present in both
181 principal piece and end piece of the flagellum (**Figure 2A, upper panel**). The distinct linear
182 CatSper nanodomain arrangement visualized by Structured Illumination Microscopy (SIM)
183 was not seen for SPINK3 in the flagellar membrane (**Figure 2B**). These observations,
184 combined with our finding that SPINK3 inhibits the processing of the N-terminal cytoplasmic
185 domain of CATSPER1, prompted us to further investigate the spatial distribution of SPINK3 in
186 relation to the plasma membrane. Thus, SPINK3 immunostaining was performed together with
187 membrane labelling using the specific plasma membrane probes FM4-64 and CellBrite.
188 Images from Airyscan microscopy and MSSR indicate that SPINK3 is externally associated
189 with the plasma membrane (**Figure 2C, Supp. Movie 1**). Accordingly, SPINK3 signal spans
190 a wider area than the measured membrane-to-membrane distances (**Figure 2C, MSSR**
191 **Images**). Nevertheless, we observed that the SPINK3 association with sperm is compromised
192 in *Catsper1* KO sperm and there is also a pattern shift (**Figure 2A (lower panel), D; Supp.**
193 **Figure 3**). It is possible that in *Catsper1* KO sperm the loss of CatSper complex from flagellum
194 changed the membrane property and/or protease localization, thus compromising the
195 attachment of SPINK3. These results suggest that SPINK3 interacts with the flagellar
196 membrane in a CatSper-dependent manner but does not directly bind to CatSper.
197
198 **SPINK3, but not SBTI, specifically affects sperm capacitation events**
199
200 Given that protection of CATSPER1 from proteolytic processing (*i.e.*, intact CATSPER-
201 mediated Ca^{2+} signaling) is required to control the timing of capacitation, we analyzed whether
202 the protease inhibitory activity of SPINK3 accounts for its function as a decapacitation factor.
203 To this end, we first tested whether the trypsin inhibitor SBTI could mimic the known effects of
204 SPINK3 on capacitation since SBTI can also inhibit CATSPER1 processing (**Supp. Figure 2**).
205 In contrast to SPINK3, there was no difference in the BSA-induced increase in $[Ca^{2+}]_i$ between
206 SBTI-treated and untreated spermatozoa as assessed by single-cell Ca^{2+} imaging with Fluo-
207 3 AM (**Figure 3A**), nor in the percentage of acrosome-reacted spermatozoa (**Figure 3B**).

Notably, neither SPINK3 nor SBTI affected intrasperm alkalinization (**Figure 3C**), which is known to increase CatSper currents (8, 27, 28). All these results suggest that among trypsin-like protease inhibitors, SPINK3 specifically inhibits capacitation events such as rise in $[Ca^{2+}]_i$ and AR likely through a mechanism distinct from its inhibition of CATSPER1 cleavage.

SPINK3 alleviates capacitation-induced membrane perturbations

Cholesterol efflux from the sperm plasma membrane is a crucial step in capacitation. These changes promote an increase in membrane fluidity or decrease stability (29) and can be measured using BODIPY-cholesterol (BODIPY/Ch), a fluorescent compound that can replace endogenous cholesterol in the membrane without disturbing the lipid acyl chain region. Therefore, its loss can be measured by changes in fluorescence intensity (30, 31). By contrast, the subsequent membrane remodeling can be assessed by the incorporation of anionic lipophilic fluorescent dye Merocyanine 540 (M540) as the amount of dye per unit surface area increases in less-ordered membranes (32, 33). Using these lipid indicators, we show that capacitated spermatozoa contain lower cholesterol content (**Figure 4A**) and increased lipid disorder (**Figure 4B**) compared to non-capacitated sperm, as previously reported. In contrast, pre-incubation with SPINK3 blocked the capacitation-associated cholesterol efflux and lipid disorder (**Figure 4A**, **B**), suggesting that SPINK3 binding to the membrane hinders the membrane reordering during capacitation.

SPINK3-exposed spermatozoa during capacitation reduce *in vitro* fertilization

Pharmacological inhibition of CatSper during *in vitro* capacitation compromises sperm fertilizing ability *in vitro* (34). *In vivo*, decapacitation factors are gradually removed from the sperm surface within the female reproductive tract, thereby allowing capacitation to proceed. In contrast, conventional *in vitro* fertilization (IVF) assays are performed with epididymal sperm, which naturally lack seminal plasma proteins such as SPINK3, and membrane-bound proteins might not be efficiently detached under these conditions. To specifically evaluate whether exogenously added SPINK3 exerts an inhibitory effect in vitro, epididymal sperm were incubated under capacitating conditions in the absence or presence of 13 μM recombinant SPINK3 and subsequently used for inseminating cumulus–oocyte complexes (COCs). We found that SPINK3 produced a significant decrease in the percentage of fertilized eggs (**Figure 5A, B**). Most sperm that were preincubated with SPINK3 retained SPINK3 immunostaining in the flagellum when recovered 4 hours after insemination (**Figure 5C**).

DISCUSSION

SPINK3 is involved in the regulation of CATSPER1 processing protease in mice

We have previously reported that the small vesicular protein SPINK3, found in mouse male secretions, acts as a decapacitation factor by inhibiting CatSper activity and the increase of $[Ca^{2+}]_i$ during the early stages of capacitation induced by BSA and HCO_3^- (18). We have also shown that SPINK3 functions as a Kazal-type serine protease inhibitor that competitively inhibits trypsin-like proteases (19). Concurrently, it has been shown that both CATSPER1 and CATSPERθ undergo capacitation-induced degradation (12, 14, 15). However, endogenous protein(s) responsible for this physiological regulation remains unidentified. In this study, we show that SPINK3 inhibits sperm trypsin-like proteases and specifically inhibits the

256 capacitation-associated cleavage of CATSPER1, but not CATSPERθ, suggesting a
257 sophisticated regulatory role for SPINK3 in controlling CatSper channel activity.

258 It has been suggested that inhibitors of calpain, a family of calcium-dependent cysteine
259 proteases, also block CATSPER1 processing (15). However, SPINK3, as a serine protease
260 inhibitor, is unlikely to directly inhibit calpains. Given that SPINK3 specifically inhibits serine
261 proteases and interferes with CATSPER1 processing, if this effect results from a direct action
262 of SPINK3 on a sperm protease, then the protease responsible for CATSPER1 cleavage is
263 likely a serine protease. Alternatively, CATSPER1 N-terminal domain cleavage could be a
264 multi-protease event involving different types of proteases. Other sperm serine proteases have
265 been reported in mouse sperm, such as ACROSIN (Q3ZB06_MOUSE), PRS55
266 (Q14BX2_MOUSE), and TESP1 (Q3U132_MOUSE), but all are localized in the sperm head,
267 either as part of the membrane fraction (GPI-anchored or transmembrane included) or soluble
268 in the acrosome. However, no protease has been described specifically in the sperm flagella,
269 where CATSPER1 processing is thought to occur. This requires further investigation.

270 **SPINK3 modulates capacitation through mechanisms that extends beyond its**
271 **protease inhibitory activity**
272
273 While the finding that SPINK3 inhibits CATSPER1 processing does not fully explain
274 the mechanism by which this protein regulates capacitation, we used soybean trypsin inhibitor
275 (SBTI) as an alternative trypsin-like protease inhibitor to further investigate this process. SBTI
276 had previously been shown to block the SPINK3 binding site on the sperm head in mouse
277 sperm (25), suggesting a potential shared target between these molecules in this region.
278 Additionally, SBTI has been used to detect acrosin exposure in other mammalian sperm (35),
279 indicating its interaction with acrosomal proteases. Given these findings, we selected SBTI to
280 determine whether inhibiting serine proteases alone is sufficient to regulate capacitation. Our
281 results show that, despite SBTI's ability to inhibit sperm proteases involved in CATSPER1
282 degradation, it does not modulate capacitation as SPINK3 does, suggesting that SPINK3's
283 role in capacitation extends beyond its inhibitory function on serine proteases.

284 Our *in vitro* results demonstrate that both SPINK3 and seminal vesicles extracts
285 (containing native SPINK3) strongly inhibit sperm trypsin-like proteases, however evidence
286 shows that SPINK3 acts extracellularly. Therefore, it is possible to consider a role for surface
287 attached SPINK3 in stabilizing the membrane and CatSper arrangements in the principal
288 piece, by binding a membrane protease, whose substrate is CATSPER1, and likely to be
289 differently compartmentalized outside of CatSper nanodomains before capacitation. Although
290 there is no strict co-localization of SPINK3 and CATSPER1, sperm from *Catsper1* KO mice,
291 which lack the entire channel complex in the spermatozoa, displayed a different SPINK3-
292 sperm binding ability and pattern, suggesting that SPINK3 binds to the sperm flagellum in a
293 CatSper dependent manner. The different and compromised SPINK3 binding with sperm may
294 be because lipid domain arrangement was disrupted due to the lack of CatSper channel in the
295 sperm flagella. Given that TESP1 has previously been reported as the ligand for SPINK3 in
296 the acrosomal region (25), it is possible that the mechanisms governing SPINK3 binding to
297 sperm vary across membrane subregions. In sperm lacking the CatSper channel—and
298 consequently exhibiting defective molecular organization along the flagellum—SPINK3
299 attachment may be restricted to the head, as the principal piece may no longer provide a

300 suitable binding site. Additionally, SPINK3 might play distinct roles in different sperm regions:
301 one regulating calcium influx to modulate hyperactivation and the other controlling the
302 acrosome reaction. However, the latter is beyond the scope of this study and requires further
303 investigation.

304 **SPINK3 might be involved in the development of sperm subpopulations in the**
305 **oviduct**

306 SPINK3 is bound to the majority of sperm during ejaculation, and it is progressively
307 detached along the oviduct; however, this detachment is asynchronous, as it does not occur
308 simultaneously in all sperm (21). Besides, it is not clear what modulates CatSper activity and
309 how CatSper channel containing N-terminally processed CATSPER1 (15) alters its activity.
310 As most sperm found in the ampulla has a molecular barcode of acrosome reacted (AR +),
311 tyrosine phosphorylation negative (pY -), and CATSPER1 intact (CATSPER1 +), and our
312 results show that pY- sperm are also SPINK3+, one can speculate that late release of SPINK3
313 from the flagellar membrane contributes to avoid premature cleavage of CATSPER1 and thus
314 premature degeneration. Proteolysis of membrane protein ectodomains acts as a post-
315 translational modification that determines the levels and activity of membrane proteins (36).
316 Would CATSPER1-cleaved sperm show increased or reduced CatSper activity? Would intact
317 CATSPER1 be maintained in the fertilizing sperm or just until right before? In this work, our
318 evidence shows that SPINK3 prevents this proteolysis that occurs in capacitating media and
319 also prevents membrane reorganization, increase in $[Ca^{2+}]_i$, and acrosome exocytosis, but it
320 is unclear whether early or late release constitutes the destiny of sperm for fertilization.
321 Recently, it has been reported that seminal plasma spermine reversibly inhibits CatSper's
322 temperature gating, protecting against premature activation (37). May heterogeneity reflects
323 a compilation of the time- and space-dependent changes that sperm undergo along the
324 oviduct? Could the importance of tightly regulating CatSper function be such that multiple
325 redundant molecules operate in parallel to ensure fertilization success? All these questions
326 serve ongoing and future research directions.

327 While SPINK3 is gradually removed from sperm surface *in vivo* in female's
328 reproductive tract (21), the detachment is less efficient *in vitro*, as evidenced by the intense
329 SPINK3 labeling in the sperm recovered from the co-culture and fertility significantly reduced,
330 suggesting that the detachment of SPINK3 from sperm needs specific physiological conditions
331 or specific molecules in female's reproductive tract.

332 In conclusion, we demonstrate a role for SPINK3 in stabilizing the membrane and
333 preventing CATSPER1 processing, either indirectly or directly acting as an inhibitor of the
334 responsible protease that cleaves CATSPER1. Our findings provide molecular insights into
335 the dynamic regulation of capacitation by male-derived SPINK3 and provide the first evidence
336 of a natural molecule involved in modulating the CatSper channel. This work helps to explain
337 the mechanism for the graded subpopulations of sperm along the female reproductive tract.

338

339 **MATERIALS AND METHODS**

340

341 ***Animals***
342
343 Female and male mice (*Mus musculus*) of BALB/c and C57BL/6 strains and sexually
344 mature (BALB/c x C57BL/6) F1 hybrids were maintained at 22°C with a photoperiod of 12 h
345 light:12 h darkness, food and water *ad libitum*. Sexually mature (2–3 months) male and female
346 mice were euthanized by cervical dislocation.
347 *Catsper1*-null mice were previously generated (7) and maintained on a C57BL/6
348 background.
349 Mice were cared for in compliance with the guidelines approved by local Animal Care
350 and Use Committees (UNMdP RD 104/22), following the National Institutes of Health Guide
351 to the Care and Use of Laboratory Animals.
352
353 ***Antibodies and reagents***
354
355 Rabbit polyclonal antibodies against CATSPER1 (7), CATSPERθ (12) and SPINK3
356 (Sigma HPA027498) were used. A monoclonal anti-HA antibody was purchased from Cell
357 Signaling Technology (#3724), and a monoclonal anti-tubulin antibody (T6094, 1:5000) was
358 obtained from Sigma-Aldrich. HRP-conjugated goat anti-rabbit IgG and goat anti-mouse IgG
359 were used as secondary antibodies. Recombinant SPINK3 protein was produced in *E. coli*
360 and purified using HiTrap IMAC HP (GE Healthcare Life Sciences).
361 Additional reagents included: Soybean Trypsin Inhibitor (SBTI) (1 μM), Fluo-3 AM
362 (Invitrogen USA, Molecular Probes, F1242), Pluronic acid (Invitrogen, USA), Laminin (100
363 μg/ml, BD Biosciences), PNA Alexa Fluor 594 lectin (1 μg/ml, Molecular Probes, L-32459),
364 Bodipy-Cholesterol (15 μM, Cayman, 24618), M540 (2.7 μM, Sigma-Aldrich, 323756), FM4-
365 64FX (100 μM, Invitrogen, F34653), CellBrite Fix 640 (2.5 μM, Biotium, 30089-T), Yo-Pro1 (50
366 nM, Invitrogen, Y3603), Trypsin (347 USP-u/mg, Biological industries, 4192025), PMSF
367 (Phenylmethylsulfonyl fluoride, 500μM, ICN Biomedicals Inc., 195381) and fluorogenic
368 protease substrates Z-CGGR-AMC (7-Amino-4-methylcoumarin), Suc-LLVY-AMC, and Z-
369 SLY-AMC (2 μM each; all from Sigma-Aldrich, Merck, Darmstadt, Germany) .
370
371 ***Expression and purification of recombinant SPINK3***
372
373 For the production of SPINK3, the cDNA encoding the mature SPINK3 from *M.*
374 *musculus* (NCBI ID: NM 009258.5) was cloned into the pET-24b(+) (Novagen, Madison, WI,
375 USA) expression vector. Overexpression of SPINK3 was performed in *Escherichia coli*
376 Rosetta cells (Novagen) and the recombinant protein was purified to apparent homogeneity
377 as described (19, and Supplementary Information S1).
378
379 ***Sperm preparation***
380
381 Epididymal spermatozoa from adult male mice were collected by swim-out from caudal
382 epididymis in M2 medium (EMD Millipore, MR-015-D) or HM medium (Modified Krebs Ringer
383 Bicarbonate medium: 20 mM Hepes, 119.3 mM NaCl, 4.7 mM KCl, 1.2 mM $MgSO_4$, 5.6 mM
384 glucose, 1.2 mM KH_2PO_4, 0.5 mM Na pyruvate and 1.7 mM $CaCl_2$; pH 7.4). Collected sperm
385 were washed with fresh HM or PBS.
386 For capacitation, sperm were incubated in HMB (HM plus 15 mM $NaHCO_3$ and 5 mg
387 mL^{-1} BSA) or human tubular fluid HTF medium (EMD Millipore, MR-070-D) at (2-7 x 10^6 cells

388 mL^{-1}) w/o purified SPINK3 at 37°C, 5% CO_2 for 1 or 2 hr. SPINK3 concentrations (5-13 μM)
389 varied according to the assay.
390 In a set of experiments capacitation was performed in the presence of SPINK3 (13 μM)
391 or SBTI (1 μM) (38, 39).
392 For the preparation of sperm lysates, sperm samples (10×10^6 cells) were
393 resuspended in 1 mL of 0.1% Triton X-100 in PBS. The suspension was sonicated three times
394 for 1 second each using a small ultracentrifuge tube. Samples were then agitated for 1 hour
395 at 4 °C, followed by centrifugation at 15,000 × g for 10 minutes at 4 °C. The supernatant was
396 collected and used immediately. Lysates were always prepared freshly before use.
397
398 ***Seminal vesicle lysates***
399
400 Seminal vesicle homogenate was prepared from seminal vesicles obtained from adult
401 male mice. The tissues were placed in ice-cold PBS (pH 7.4) and homogenized using a IKA
402 T10 basic homogenizer under cold conditions. The homogenate was then centrifuged at
403 10000 × g for 10 minutes, and the supernatant was filtered (0.22μm) and stored on ice until
404 use. The homogenate was subsequently used in activity assays, adjusting the volume based
405 on the estimated concentration of native SPINK3 in seminal vesicle extracts.
406
407 ***Proteolytic activity of sperm lysates and inhibitory assay***
408
409 Proteolytic activity of sperm lysates was assessed over fluorogenic substrates: Z-Arg-
410 Gly-Arg-AMC (for trypsin-like proteases), Suc-LLVY-AMC (for chymotrypsin-like proteases),
411 and Z-SLY-AMC (for elastase-like proteases), each at a final concentration of 2 μM. All
412 reactions were performed in 96-well black plates (Nunc) with a final volume (Fv) of 100 μl per
413 well.
414 Reaction mixtures were prepared at room temperature with 40 μl of sperm lysate as
415 protease source. The reactions (Fv=100 μl) contained 50 mM Buffer phosphate pH 7.4, w/o
416 the following inhibitors: SPINK3 (1.3 μM final), SBTI (2 μg/ml final), seminal vesicle
417 homogenate as a control of native SPINK3 (6 μl) and PMSF (500 μM). The reaction was
418 initiated by adding 2 μM CGGR-AMC substrate, and fluorescence (Ex 355 nm / Em 436 nm)
419 was measured every minute for 30 min at 37 °C with agitation (Fluoroskan Ascent microplate
420 reader, Thermo Electron Corporation, Waltham, MA, USA). Blank reaction was conducted
421 including 40 μl 0,1% Triton. Enzymatic activity was calculated as Δfluorescence over time and
422 expressed relative to the sperm lysate fluorescence. Inhibition is evidenced as a decrease in
423 proteolytic activity.

424 ***In vivo proteolysis of CATSPER1***

425 Capacitation was performed w/o 13 μM SPINK3 or 1 μM SBTI for 2hrs in HTF media.
426 Western blots with whole sperm lysates (1 or 2 x 10^6 cells/lane) were performed and
427 developed with anti-CATSPER1 (7), anti-CATSPERθ (12), anti-HA (CST, #3724) or anti-
428 acetylated Tubulin (Sigma, T7451), followed by the corresponding HRP-conjugated goat anti-
429 rabbit or anti-mouse IgG.
430
431 ***In vitro proteolysis of CATSPER1***

432 HEK293T cells were transiently transfected with construct encoding CATSPER1-HA
433 with Lipofectamine 2000 (Invitrogen), following the manufacturer's instruction. CATSPER1-
434 HA was solubilized with 0.1% Triton X-100 PBS (PBST) buffer, containing EDTA-free protease
435 inhibitor cocktail and pulled-down with anti-HA magnetic beads (Pierce, 88836) for 1 h. at RT.
436 The enriched CATSPER1-HA protein beads were incubated with 30µL of sperm lysates
437 solubilized from $3.0x10^5$ sperm cells w/o 13 µM SPINK3 at 37ºC for the indicated times. After
438 incubation, the mixture was denatured by LDS sampling buffer supplemented with 50 mM DTT
439 at 75ºC for 15 min. Western Blot was performed as described before.

440

441 ***Time-lapse live cell calcium Imaging***

442

443 Mouse epididymal spermatozoa (n=3) (10 x 10^6 cells/ml) were loaded with Fluo-3 AM
444 (10 µM) (Invitrogen USA, Molecular Probes F1242) and 0.02% (v/v) pluronic acid (Invitrogen,
445 USA) as a surfactant at 37°C for 20 minutes in a non-capacitating medium (NC). Non-
446 capacitated sperm were then incubated w/o SPINK3 (13 µM) or SBTI (1 µM) for 15 minutes
447 at 37°C and then, adhered to a fluorescence compatible 96 well plate previously covered with
448 laminin (100 µg/ml, BD Biosciences). HM medium supplemented with 15 mM $NaHCO_3$ was
449 added to the chamber and basal fluorescence was monitored under confocal microscope
450 (excitation 488 nm; emission 526 nm, Nikon C1SiR) at 400x magnification. BSA (5 mg/ml) in
451 a minimum volume was applied, and changes in the calcium signal were recorded throughout
452 the process. The viability of the spermatozoa was determined through the motility of the
453 flagellum. The intensity of the fluorescence signal in the head of spermatozoa with motile
454 flagella was quantified using the free software ImageJ 1.43 (National Institutes of Health,
455 Bethesda, Maryland, United States). Data was normalized using the equation (F-F0)/F0,
456 where F is the fluorescence intensity at time t and F0 is the mean fluorescence taken during
457 the period before the addition of BSA (initial 10 seconds). Then, the total series of (F-F0)/F0
458 was plotted against time, as well as the percentage of positive response to the stimulus.

459

460 ***Acrosomal reaction (AR) assay***

461

462 Mouse epididymal spermatozoa (n=3) were capacitated (7.5 x 10^6 cells/ml) for 60
463 minutes w/o SPINK3 (13 µM) or SBTI (1 µM). To induce the acrosomal reaction, spermatozoa
464 were incubated with progesterone (50 µM) (18) or Ca^{2+} ionophore A23187 (10 µM) (Sigma-
465 Aldrich, United States) for 15 min at 37°C after capacitation. The cells were then incubated for
466 15 minutes at 37°C with the PNA Alexa fluor 594 lectin (1 µg/ml, Molecular Probes, L-32459),
467 which allows AR to be detected by binding to glycoproteins of the internal acrosomal
468 membrane. The fluorescence was observed under a microscope at a magnification of 400x.
469 Sperm that lost their acrosomes (red fluorescence) were expressed as a percentage of 100
470 cells per replicate.

471

472 ***Cholesterol efflux assay***

473

474 Mouse epididymal spermatozoa (n=3) (15 x 10^6 cells/ml) were loaded with Bodipy-
475 Cholesterol (15 µM) (Cayman, 24618) for 30 minutes at 37°C and incubated 15 minutes at
476 37°C w/o SPINK3 (13 µM) or SBTI (1 µM). Cells were washed to remove excess reagent and
477 exposed for 60 minutes to either capacitation (CAP) or non-capacitation (NC) conditions. The
478 fluorescence of the labeled Bodipy cholesterol was observed in a Nikon Eclipse T2000

479 epifluorescence microscope with a magnification of 400x, and the percentage of cells that
480 preserved the labeled cholesterol was quantified.
481
482 ***Determination of lipid disorder***
483
484 Mouse epididymal sperm (n=3) ($10x10^6$ cells/ml) were incubated in the presence or
485 absence of rSPINK3 (13 µM) for 15 minutes at 37°C in HM medium. Subsequently, they were
486 incubated under CAP or NC conditions. After capacitation, 2.7 µM M540 (Ex 555/Em 578 nm,
487 Sigma-Aldrich, 323756) was added to the sperm suspension ($1x10^6$ total cells) and incubated
488 for 15 minutes at room temperature in the dark. Cells were washed and Yo-Pro1 was added
489 at a concentration of 50 nM (Ex 491/Em 509 nm., Invitrogen, Y3603). The samples were
490 analyzed by flow cytometry. The results were analyzed using the open access Flowing 2
491 software. During acquisition, sperm were discriminated from debris. The results are expressed
492 as the percentage of cells with lipid disorder over the total live cells (M540+/Yo-Pro1-).
493
494 ***Immunolabeling of SPINK3 and CATSPER1***
495
496 Epididymal spermatozoa from WT and *Catpser1*-/- mice (n=3) were incubated in non-
497 capacitating medium w/o SPINK3 (13 µM) for 15 minutes at 37°C. Each condition was
498 centrifuged twice at 500 × g for 5 minutes, and re-suspended in the same volume of fresh PBS
499 medium without SPINK3. Cells were seeded on 8-well glass slides and allowed to air-dry.
500 Sperm were fixed with 3.7% paraformaldehyde in PBS for 15 minutes at room temperature,
501 washed with PBS and permeabilized with 0.5% Triton X-100 for 5 minutes. After washing with
502 PBS, cells were blocked with 5% BSA in PBS for 1 h at room temperature and followed by
503 overnight incubation with anti-SPINK3 (1:50 in TBS supplemented with 1 % BSA and 0.1 %
504 tween, Sigma HPA027498) at 4 °C. After washing with PBS, anti-rabbit IgG-Alexa 488
505 (1:1000, Abcam, ab15105) was added for 2 hours at room temperature. Finally, the cells were
506 washed with PBS and mounted to acquire images with the fluorescence microscope NIKON
507 ECLIPSE E800. Images from both conditions (WT and *Catpser1*-/-) were equally processed
508 and analyzed with ImageJ (v1.38, NIH). For data analysis, the percentage of SPINK3-positive
509 sperm under each condition was adjusted by subtracting the count of false positive sperm
510 observed in the basal immunofluorescence controls (i.e., WT or *Catpser1*-/- sperm incubated
511 without SPINK3).
512 To assess tyrosine-phosphorylated proteins (anti-pY), sperm were incubated w/o
513 SPINK3 (13 µM), incubated under CAP or NC conditions and then the cells were fixed with
514 4% formaldehyde, washed, and placed on slides. Once dried, they were fixed with 96%
515 ethanol, permeabilized with 10 µl of T-PBS (1x PBS, 0.5% Tween 20%) with 0.5% Triton 100
516 for 20 minutes. After washing, they were blocked with 3% BSA in T-PBS for 1 hour. The
517 samples were washed and incubated for 1 hour with the primary antibody anti-tyrosine mouse
518 monoclonal (anti-pY) (1:500, Clone 4G10, Millipore) or anti-SPINK3 (1:50, Sigma Aldrich,
519 HPA027498) in blocking buffer, followed by the secondary antibodies anti-rabbit IgG-Alexa488
520 (1:1000, Invitrogen A11070) and anti-mouse IgG-Alexa455 (1:500, Invitrogen, A21425). The
521 preparations were mounted with glycerol:PBS (9:1) and observed under a fluorescence
522 microscope with a magnification of 400x (Ex 480/Em 525 nm).

523 ***Structured illumination microscopy***

524 2D structured illumination microscopy (SIM) imaging was performed with Zeiss
525 LSM710 Elyra P1 using alpha Plan-APO 100X/1.46 oil objective lens. Samples were prepared
526 as described in the previous section (Sperm labelling with SPINK3 and immunostaining with
527 CATSPER1 antibody). Raw images were processed and rendered using Zen 2012 SP2
528 software (Carl Zeiss).

529 ***Plasma membrane labeling***

530

531 After obtaining the sperm sample and co-incubating it with SPINK3 as previously
532 described, the sample was incubated with 100 µM FM4-64 FX for 3 minutes at room
533 temperature or with 2.5 µM CellBrite Fix 640 for 15 minutes at 37°C, followed by the SPINK3
534 immunolabeling protocol as described above. Confocal images were acquired using a Zeiss
535 LSM-880 microscope equipped with an Alpha Plan-Apochromat 100x/1.46 objective. Images
536 were also captured in Super-Resolution mode using an Airyscan detector. A total of 10 frames
537 were acquired, and the Mean-Shift Super Resolution (MSSR) algorithm (40) was applied to
538 enhance resolution.

539

540 ***In vitro fertilization***

541

542 F1 hybrid females (female Balb/c x male C57BL/6) were superovulated by
543 intraperitoneal injection with 7.5U of PMSG and 48 hours later with 5U of hCG. Cumulus-
544 oocyte complexes (COCs) were obtained from the ampulla 15 hours post hCG and placed in
545 G-IVF plus medium droplets (LifeCell) under mineral oil (M8410, Sigma-Aldrich).
546 Subsequently, groups of COCs were transferred to a clean medium drop (90 µl) under oil.
547 Spermatozoa were obtained from C57BL/6 males in HM medium, incubated w/o SPINK3 (13
548 µM) for 15 minutes at 37°C and capacitated in G-IVF plus medium (LifeCell) (5 x 10^6 cells/ml).
549 COCs were inseminated with 10 µl of the sperm suspension and incubated at 37°C, 5% CO2
550 for 4 hours. Afterward, COCs were washed, and putative zygotes were incubated for 24 hours
551 and 5 days (post-IVF) to assess the two-cell and blastocyst stages under an inverted
552 microscope with a magnification of 400x (Nikon Eclipse Ti-S). Remanent sperm were prepared
553 for immunostaining. Bar charts show the percentage of two-cell embryos and blastocysts over
554 the total fertilized oocytes.

555 ***Statistical analysis***

556

557 Data were analyzed by GLMM (generalized linear mixed effect model) to determine
558 statistical significance between treatments and control (41). The model included the male
559 variable as a random effect. Normality of residuals was assessed by plotting theoretical
560 quantiles vs standardized residuals (Q–Q plots). Homogeneity of variance was evaluated by
561 plotting residuals vs fitted values. A post hoc analysis was conducted with the 'lsmeans''
562 package (42). In all cases, the analysis was performed using R software version 3.3.33, with
563 the 'nlme' package for Gaussian models (43). Statistically significant differences were
564 determined at $P < 0.05$. Graph bars indicate mean ± s.e.

565

Declaration of interest

The authors declare that there is no conflict of interest that could be perceived as prejudicing the impartiality of the research reported.

Funding

This work was supported by the National Scientific and Technical Research Council (CONICET, Argentina, PIP 11220200100850CO) awarded to A.C., the National Institutes of Health (R01HD096745) to J.-J.C, the Chan Zuckerberg Initiative (2021-240504), the National Institutes of Health (R01HD106968), and the Agencia Nacional de Promoción de la Investigación, el Desarrollo Tecnológico y la Innovación (Argentina, 2020-00988) to M.G.B, and grants PICT 2019-1779 and PICT 2021-0102 to D.K.. X.H. is a postdoctoral fellowship awardee of Male Contraceptive Initiative (MCI).

Data availability statement

All datasets used for this study are available upon request.

Author contribution statement

AC and JJ contributed to the conceptualization of the study and supervision. AN, XH, CS, GD, AR and LG contributed to the design and development of the methodology. AN, XH, DK, MB, LZ, AC and JJ contributed to the writing and editing of the manuscript. All the co-authors were involved in the formal analysis, validation, visualization of the results and revised the manuscript.

Acknowledgements

The authors would like to thank Viviana Daniel for their assistance during confocal microscopy. The authors also acknowledge Hugo Nuñez for his assistance with the animal handling and maintenance.

REFERENCES

1. A. R. Nicolli, A. Cesari, The other side of capacitation: role of mouse male molecules in the regulation of time and place of capacitation. *Reproduction* **166** (2023). DOI: 10.1530/REP-23-0188.
2. M. C. Chang, Fertilizing capacity of spermatozoa deposited into the fallopian tubes [9]. *Nature* [Preprint] (1951). DOI: 10.1038/168697a0.
3. C. R. AUSTIN, The capacitation of the mammalian sperm. *Nature* **170** (1952). DOI: 10.1038/168697b0.
4. W. R. Dukelow, H. N. Chernoff, W. L. Williams, Properties of decapacitation factor and presence in various species. *J Reprod Fertil* **14** (1967). DOI: 10.1530/jrf.0.0140393.
5. T. Leahy, B. M. Gadella, Sperm surface changes and physiological consequences induced by sperm handling and storage. *Reproduction* [Preprint] (2011). DOI: 10.1530/REP-11-0310
6. J. Y. Hwang, J. J. Chung, CatSper Calcium Channels: 20 Years On. *Physiology* [Preprint] (2023). DOI: 10.1101/2024.11.18.624146.
7. D. Ren, *et al.*, A sperm ion channel required for sperm motility and male fertility. *Nature* **413** (2001). DOI: 10.1038/35098027.

612 8. Y. Kirichok, B. Navarro, D. E. Clapham, Whole-cell patch-clamp measurements of
613 spermatozoa reveal an alkaline-activated Ca2+ channel. *Nature* **439** (2006). DOI:
614 10.1038/nature04417.
615 9. T. A. Quill, *et al.*, Hyperactivated sperm motility driven by CatSper2 is required for
616 fertilization. *Proc Natl Acad Sci U S A* **100** (2003). DOI: 10.1073/pnas.2136654100.
617 10. H. Qi, *et al.*, All four CatSper ion channel proteins are required for male fertility and
618 sperm cell hyperactivated motility. *Proc Natl Acad Sci U S A* **104** (2007). DOI:
619 10.1073/pnas.0610286104.
620 11. J. J. Chung, B. Navarro, G. Krapivinsky, L. Krapivinsky, D. E. Clapham, A novel gene
621 required for male fertility and functional CATSPER channel formation in spermatozoa.
622 *Nat Commun* **2** (2011). DOI: 10.1016/j.bpj.2010.12.698.
623 12. X. Huang, *et al.*, A CUG-initiated CATSPERθ functions in the CatSper channel
624 assembly and serves as a checkpoint for flagellar trafficking. *Proc Natl Acad Sci U S A*
625 **120** (2023). DOI: 10.1073/pnas.2304409120
626 13. J. Y. Hwang, Analysis of Ca2+-mediated sperm motility to evaluate the functional
627 normality of the sperm-specific Ca2+ channel, CatSper. *Front Cell Dev Biol* **12** (2024).
628 DOI: 10.3389/fcell.2024.1284988.
629 14. J. J. Chung, *et al.*, Structurally distinct Ca2+ signaling domains of sperm flagella
630 orchestrate tyrosine phosphorylation and motility. *Cell* **157** (2014). DOI:
631 10.1016/j.cell.2014.02.056.
632 15. L. Ded, J. Y. Hwang, K. Miki, H. F. Shi, J. J. Chung, 3D in situ imaging of female
633 reproductive tract reveals molecular signatures of fertilizing spermatozoa in mice. *Elife*
634 **9** (2020). DOI: 10.7554/eLife.62043.
635 16. A. Dematteis, S. Miranda, … M. N.-B. of, undefined 2008, Rat caltrin protein modulates
636 the acrosomal exocytosis during sperm capacitation. *academic.oup.com*. DOI:
637 10.1095/biolreprod.107.067538.
638 17. R. Tiwari, *et al.*, Androgen deprivation upregulates SPINK1 expression and potentiates
639 cellular plasticity in prostate cancer. *Nat Commun* **11** (2020). DOI: 10.1038/s41467-
640 019-14184-0.
641 18. L. Zalazar, *et al.*, Male Decapacitation Factor SPINK3 Blocks Membrane
642 Hyperpolarization and Calcium Entry in Mouse Sperm. *Front Cell Dev Biol* **8** (2020).
643 DOI: 10.3389/fcell.2020.575126.
644 19. D. M. Assis, *et al.*, Novel inhibitory activity for serine protease inhibitor Kazal type-3
645 (Spink3) on human recombinant kallikreins. *ingentaconnect.com* **20**, 1098–1107
646 (2013). DOI: 10.2174/0929866511320100003.
647 20. H. Lin, C. Luo, C. Wang, Y. C.-B. and Biophysical, undefined 2006, Epitope topology
648 and removal of mouse acrosomal plasma membrane by P12-targeted
649 immunoaggregation. *Elsevier*. DOI: 10.1016/j.bbrc.2006.08.045.
650 21. A. Nicolli, C. Alonso, C. Otamendi, … M. C.-, undefined 2022, How, where and when is
651 SPINK3 bound and removed from mouse sperm? *rep.bioscientifica.com*. DOI:
652 10.1530/REP-21-0195
653 22. A. A. S. Silva, *et al.*, Dissecting EPPIN protease inhibitor domains in sperm motility and
654 fertilizing ability: Repercussions for male contraceptive development. *Mol Hum Reprod*
655 **27** (2021). DOI: 10.1093/molehr/gaab066.
656 23. M. Lin, *et al.*, SPINKL, a Kazal-type serine protease inhibitor-like protein purified from
657 mouse seminal vesicle fluid, is able to inhibit sperm capacitation. *rep.bioscientifica.com*.
658 DOI: 10.1530/REP-07-0375.

24. J. Li, J. Roca, C. Pérez-Patiño, … I. B.-A. reproduction, undefined 2018, Is boar sperm freezability more intrinsically linked to spermatozoa than to the surrounding seminal plasma? *Elsevier*. DOI: 10.1016/j.anireprosci.2018.05.002.
25. S. Ramachandran, … R. B.-M. H., undefined 2021, A mouse testis serine protease, TESP1, as the potential SPINK3 receptor protein on mouse sperm acrosome. *academic.oup.com*. DOI: 10.1093/molehr/gaab059.
26. A. Cesari, M. de los Angeles Monclus, G. P. Tejón, M. Clementi & M. W. Fornes, Regulated serine proteinase lytic system on mammalian sperm surface: There must be a role. *Theriogenology*, **74** (2010). DOI: 10.1016/j.theriogenology.2010.03.029.
27. J. J. Ferreira, P. Lybaert, L. C. Puga-Molina, C. M. Santi, Conserved Mechanism of Bicarbonate-Induced Sensitization of CatSper Channels in Human and Mouse Sperm. *Front Cell Dev Biol* **9** (2021). DOI: 10.3389/fcell.2021.733653.
28. J. Y. Hwang, *et al.*, Dual Sensing of Physiologic pH and Calcium by EFCAB9 Regulates Sperm Motility. *Cell* **177** (2019). DOI: 10.1016/j.cell.2019.03.047.
29. F. M. Flesch, *et al.*, Bicarbonate stimulated phospholipid scrambling induces cholesterol redistribution and enables cholestrol depletion in the sperm plasma membrane. *J Cell Sci* **114** (2001). DOI: 10.1242/jcs.114.18.3543.
30. S. Sankaranarayanan, *et al.*, A sensitive assay for ABCA1-mediated cholesterol efflux using BODIPY-cholesterol. *J Lipid Res* **52** (2011). DOI: 10.1194/jlr.D018051.
31. N. C. Bernecic, *et al.*, BODIPY-cholesterol can be reliably used to monitor cholesterol efflux from capacitating mammalian spermatozoa. *Sci Rep* **9** (2019). DOI: 10.1038/s41598-019-45831-7.
32. L. McEvoy, R. A. Schlegel, P. Williamson, B. J. Del Buono, Merocyanine 540 as a flow cytometric probe of membrane lipid organization in leukocytes. *J Leukoc Biol* **44** (1988). DOI: 10.1002/jlb.44.4.363.
33. D. Steckler, T. A. E. Stout, C. Durandt, J. O. Nöthling, Validation of merocyanine 540 staining as a technique for assessing capacitation-related membrane destabilization of fresh dog sperm. *Theriogenology* **83** (2015). DOI: 10.1016/j.theriogenology.2015.01.019.
34. L. Curci, G. Carvajal, V. Sulzyk, S. N. Gonzalez, P. S. Cuasnicú, Pharmacological Inactivation of CatSper Blocks Sperm Fertilizing Ability Independently of the Capacitation Status of the Cells: Implications for Non-hormonal Contraception. *Front Cell Dev Biol* **9** (2021). DOI: 10.3389/fcell.2021.686461.
35. S. Sumigama, *et al.*, Progesterone accelerates the completion of sperm capacitation and activates catsper channel in spermatozoa from the rhesus macaque. *Biol Reprod* **93** (2015). DOI: 10.1095/biolreprod.115.129783.
36. S. F. Lichtenthaler, M. K. Lemberg, R. Fluhrer, Proteolytic ectodomain shedding of membrane proteins in mammals—hardware, concepts, and recent developments. *EMBO J* **37** (2018). DOI: 10.15252/embj.201899456.
37. D. K. Swain, C. Vergara, J. Castro-Arnau, Lishko, P. V., The essential calcium channel of sperm CatSper is temperature-gated. *Nature communications,* **16** (2025). DOI: 10.1038/s41467-025-58824-0.
38. L. Samanta, R. Parida, T. R. Dias, A. Agarwal, The enigmatic seminal plasma: A proteomics insight from ejaculation to fertilization. *Reproductive Biology and Endocrinology* [Preprint] (2018). DOI: 10.1186/s12958-018-0358-6.
39. T. Noda, M. Ikawa, Physiological function of seminal vesicle secretions on male fecundity. *Reprod Med Biol* [Preprint] (2019). DOI: 10.1002/rmb2.12282.

40. E. Torres-García, *et al.*, Extending resolution within a single imaging frame. *Nat Commun* **13** (2022). DOI: 10.1038/s41467-022-34693-9.
41. Zuur, *Mixed Effects Models and Extensions in Ecology with R by Zuur* (2019).
42. R. V. Lenth, Least-squares means: The R package lsmeans. *J Stat Softw* **69** (2016). DOI: 10.18637/jss.v069.i01
43. J. Pinheiro, *et al.*, Package nlme: Linear and Nonlinear Mixed Effects Models. *R package* (2020). https:// CRAN.R-project.org/package=nlme.

759 **FIGURES AND LEGENDS**
760
761

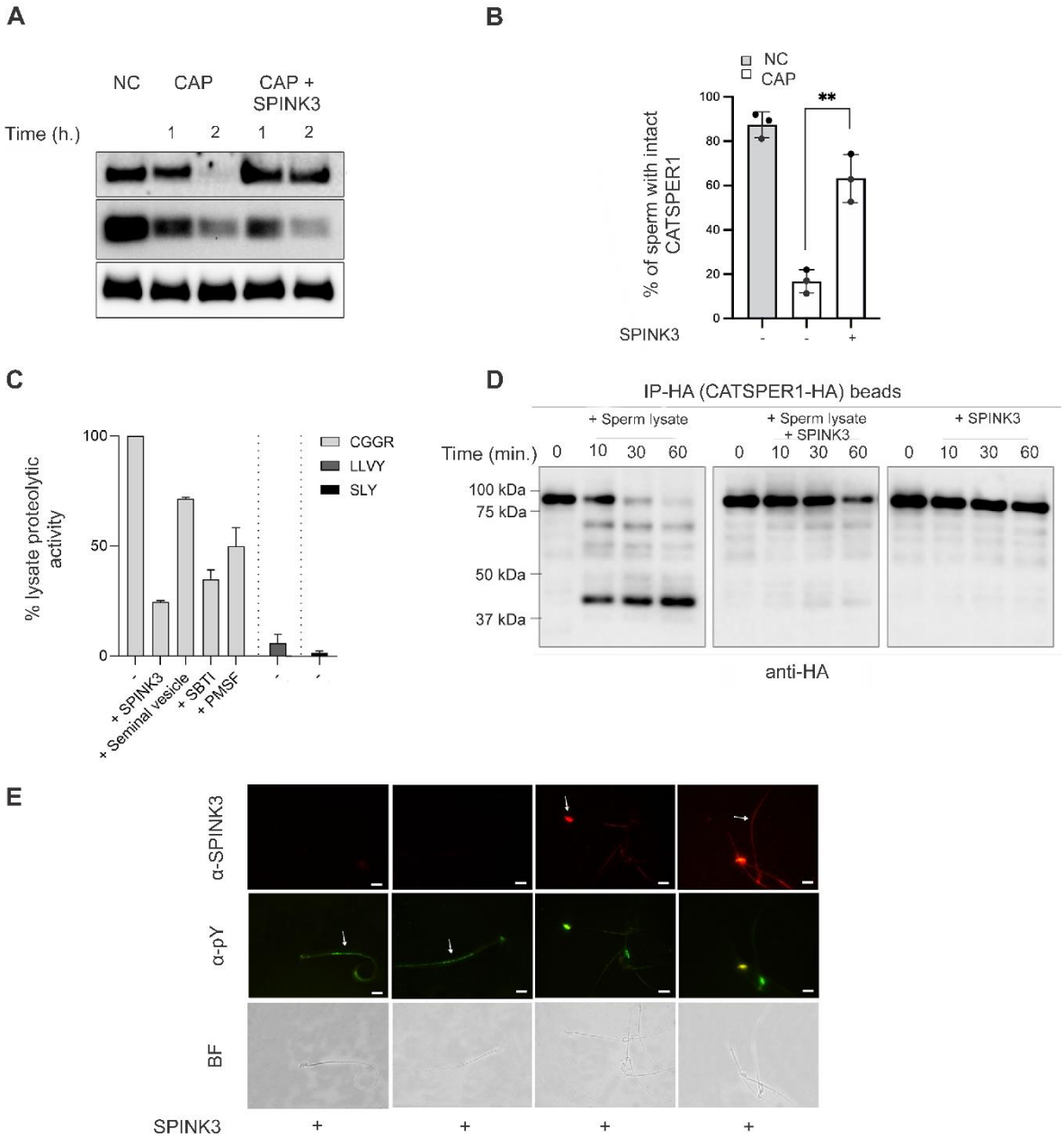

762
763
764 **Figure 1. Capacitation-induced CATSPER1 processing by sperm proteases is inhibited**
765 **by SPINK3 *in vitro*. A)** Mouse epididymal spermatozoa were incubated w/o SPINK3 (13 μM)
766 and exposed to capacitating conditions for either 1 or 2 hr., as indicated. Immunoblot analysis
767 of non-capacitated (NC) or capacitated (CAP) sperm lysates was performed with anti-
768 CATSPER1 antibody raised against the 1–150 aa region of CATSPER1 (7) and anti-
769 CATSPERθ antibody, raised against the C-terminus of CATSPERθ (12). Acetylated tubulin
770 (AC-TUB) was probed as loading control (n=3). **B)** Immunostaining with anti-CATSPER1
771 antibody was performed on non-capacitated sperm or capacitated sperm that were previously
772 incubated w/o SPINK3 for 30 min. Sperm with intact CATSPER1 signal were quantified (n=3).
773 **$p < 0.001$. **C)** Proteolytic activity of sperm lysates was measured over three fluorogenic
774 substrates—Z-Arg-Gly-Arg-AMC (CGGR; trypsin substrate), Suc-LLVY-AMC (LLVY;
775 chymotrypsin substrate), and Z-SLY-AMC (SLY; elastase substrate) in the presence or
776 absence of SPINK3 (13 μM), seminal vesicle homogenate (native SPINK3 source), SBTI

(soybean trypsin inhibitor) (2 μg/ml), or PMSF (500μM) (serine protease inhibitor) (n=3). Enzymatic activity was calculated as Δfluorescence over time and expressed relative to the sperm lysate. **D)** FL-CATSPER1-HA was expressed in 293T cells and pulled-down using magnetic beads conjugated with anti-HA antibody. The recombinant protein was then incubated with sperm lysates w/o SPINK3 (13 μM) at 37℃ for 0, 10, 30, or 60 min and subjected to immunoblot with anti-HA antibody. **E)** Tyrosine phosphorylated proteins and sperm-bound SPINK3 were detected by immunofluorescence, with anti-pY (clone 4G10, green) and anti-SPINK3 (HPA027498, red) antibodies, respectively. Arrows indicate spermatozoa exclusively stained with anti-pY or anti-SPINK3. Scale bar: 10 μm.

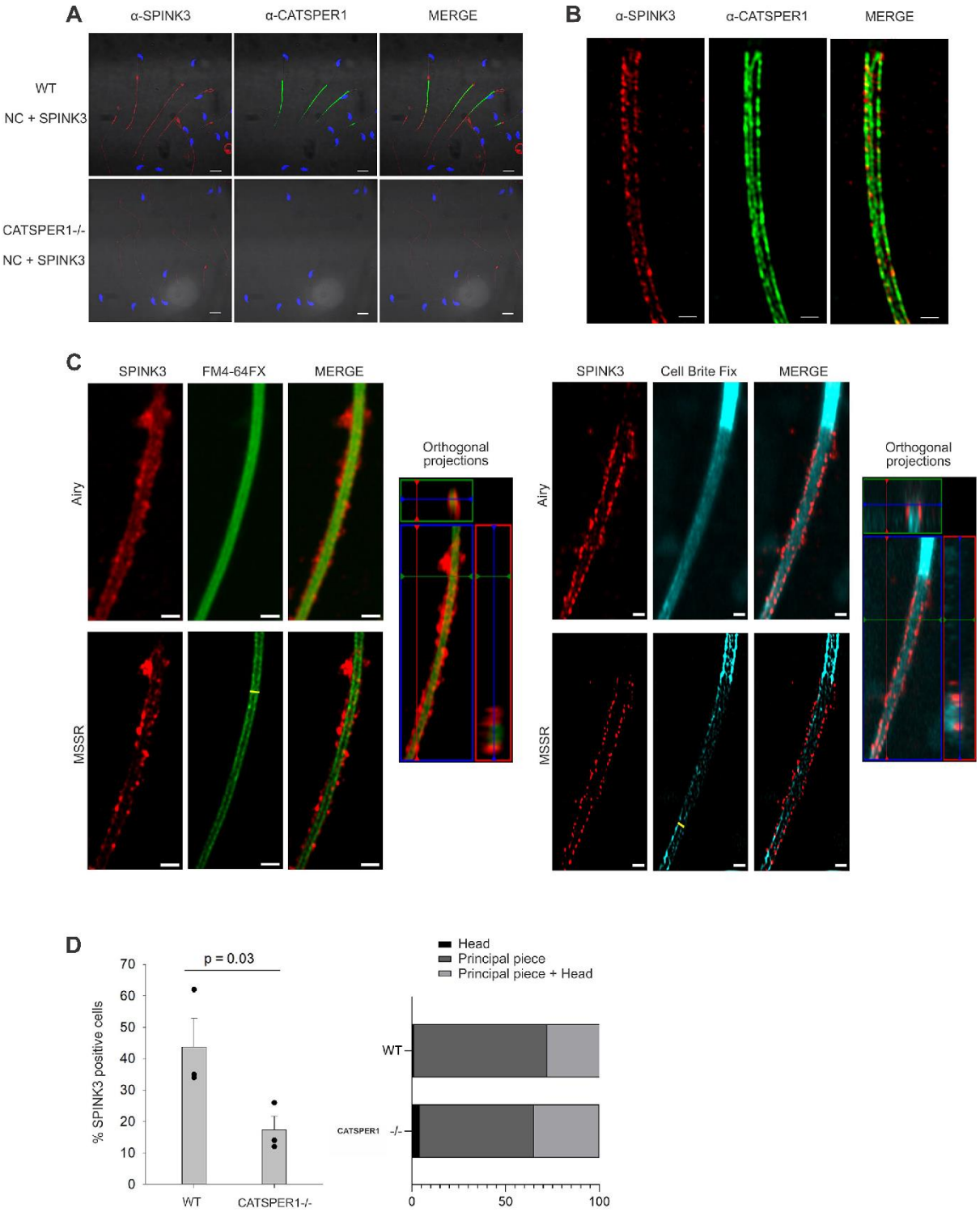

Figure 2. Immunodetection of recombinant SPINK3 binding to epididymal spermatozoa in wild type (WT) and *Catsper1* KO (*Catsper1-/-*) mice. A) Non-capacitated (NC) epididymal spermatozoa from WT and *Catsper1*-/- mice (n=3) were preincubated with SPINK3 (5 µM), and immunostaining was performed to detect SPINK3 (red) and CATSPER1 (green). Nuclei were counterstained with Hoechst (blue). Representative images from three independent experiments are shown. Scale bar: 10 µm. **B)** 2D Structured illumination microscopy (SIM) images reveal the plasma membrane localization of SPINK3 (red) on the WT NC sperm cells. The immunostaining of CATSPER1 (green) was used to indicate the boundary of the plasma

membrane. Three of the four lines of CatSper nanodomains (as indicated by CATSPER1, green) were seen in this confocal microscopy image. **C)** (Left panel) Airyscan- and MSSR-processed images show SPINK3 (red) localized on the plasma membrane of the sperm principal piece, labeled with FM4-64 FX (green). At the level of the yellow line in the FM4-64 FX MSSR image, the distance measured for FM4-64 FX is 0.409 µm, whereas for SPINK3, it is 0.736 µm. Orthogonal projections from a Z-stack are shown. Scale bar: 1 µm. (Right panel) Airyscan- and MSSR-processed images show SPINK3 (red) on the plasma membrane of the sperm principal piece, labeled with CellBrite Fix (cyan). The midpiece plasma membrane exhibits stronger staining than the principal piece. At the level of the yellow line in the CellBrite FixMSSR image, the distance measured for CellBrite is 0.442 µm, whereas for SPINK3, it is 0.752 µm. Orthogonal projections from a Z-stack are shown. Scale bar: 1 µm. **D)** (Left panel) Quantification of SPINK3-positive cells in WT and *Catsper1*-/- spermatozoa, analyzing both head and tail labeling. Data represent the mean ± SEM (n=3). Significant differences ($p < 0.05$) between WT and *Catsper1*-/- groups are indicated. (Right panel) Distribution of SPINK3 labeling in spermatozoa head and tail regions, expressed as percentages for WT and *Catsper1*-/- samples.

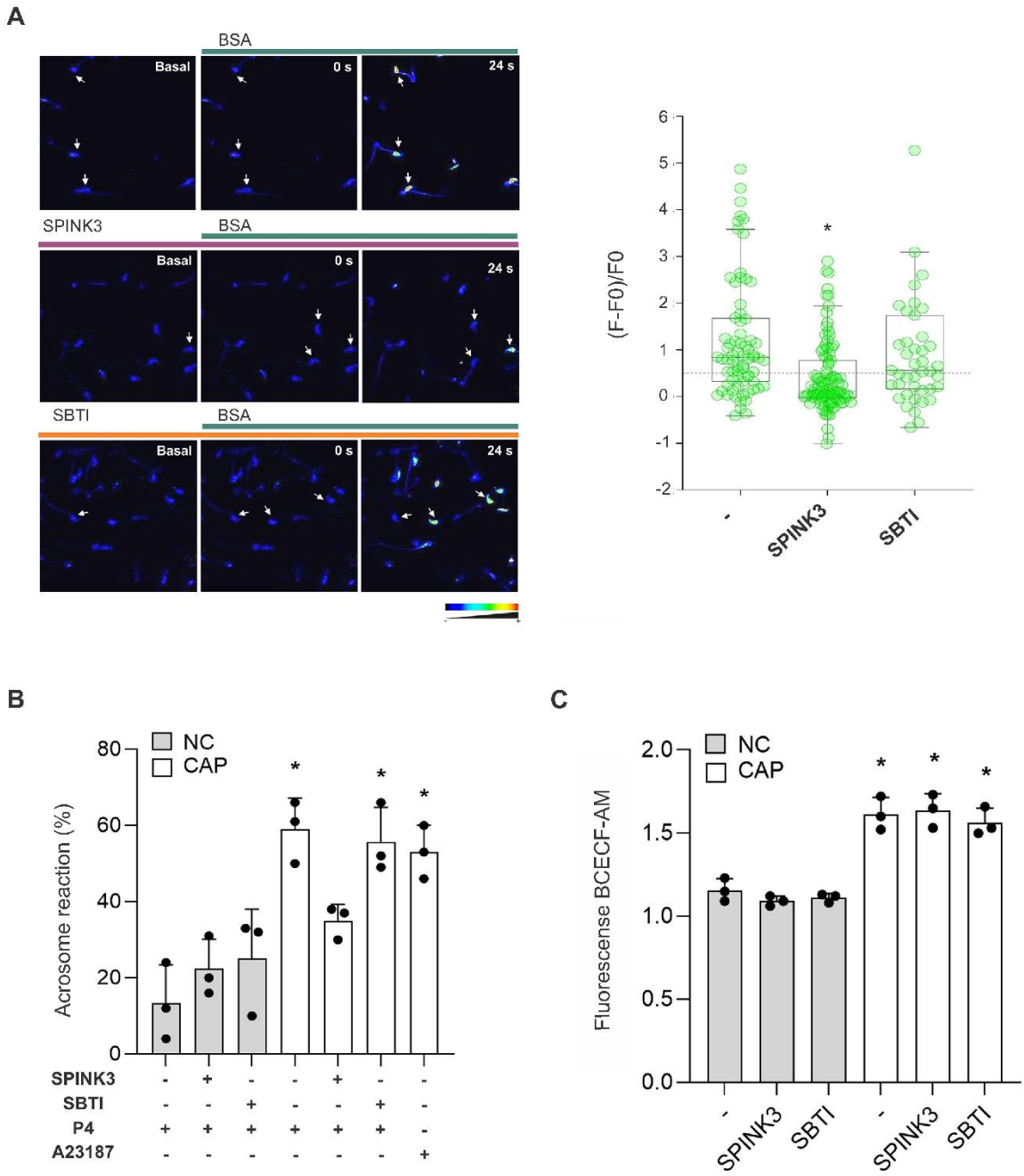

Figure 3. The inhibitory effect of SPINK3 on capacitation is not mimicked by a standard trypsin inhibitor A) Non-capacitated (NC) sperm loaded with Fluo-3 AM were exposed to SPINK3 (13 μM) or SBTI (1 μM). After washing with fresh media containing $NaHCO_3$, sperm cells were attached on laminin-coated slides and calcium signal (F0) was monitored before and after BSA was added (left panels). The fluorescence increments of individual live cells (F-F0)/F0 after 24 sec after BSA addition were plotted for each condition: control (-), SPINK3 or SBTI (right panels). *$p < 0.05$ significant differences in the percentage of responsive cells (>0.5 fold), compared to control untreated sperm. **B)** Acrosome reaction was induced by 50 μM progesterone (P4) after capacitation. As control, NC sperm cells were incubated with the Ca^{2+} ionophore A23187 (10 μM). Data represent mean ± SE; N = 3. *$p < 0.05$ significant differences compared to NC sperm. **C)** Cells under capacitating (CAP, 60 min) or non-capacitating (NC)

824 conditions were loaded with the pH-sensitive probe BCECF-AM (2 μM), and fluorescence was
825 measured (Ex 520/Em 605 nm). *p < 0.05 significant differences compared to NC sperm.

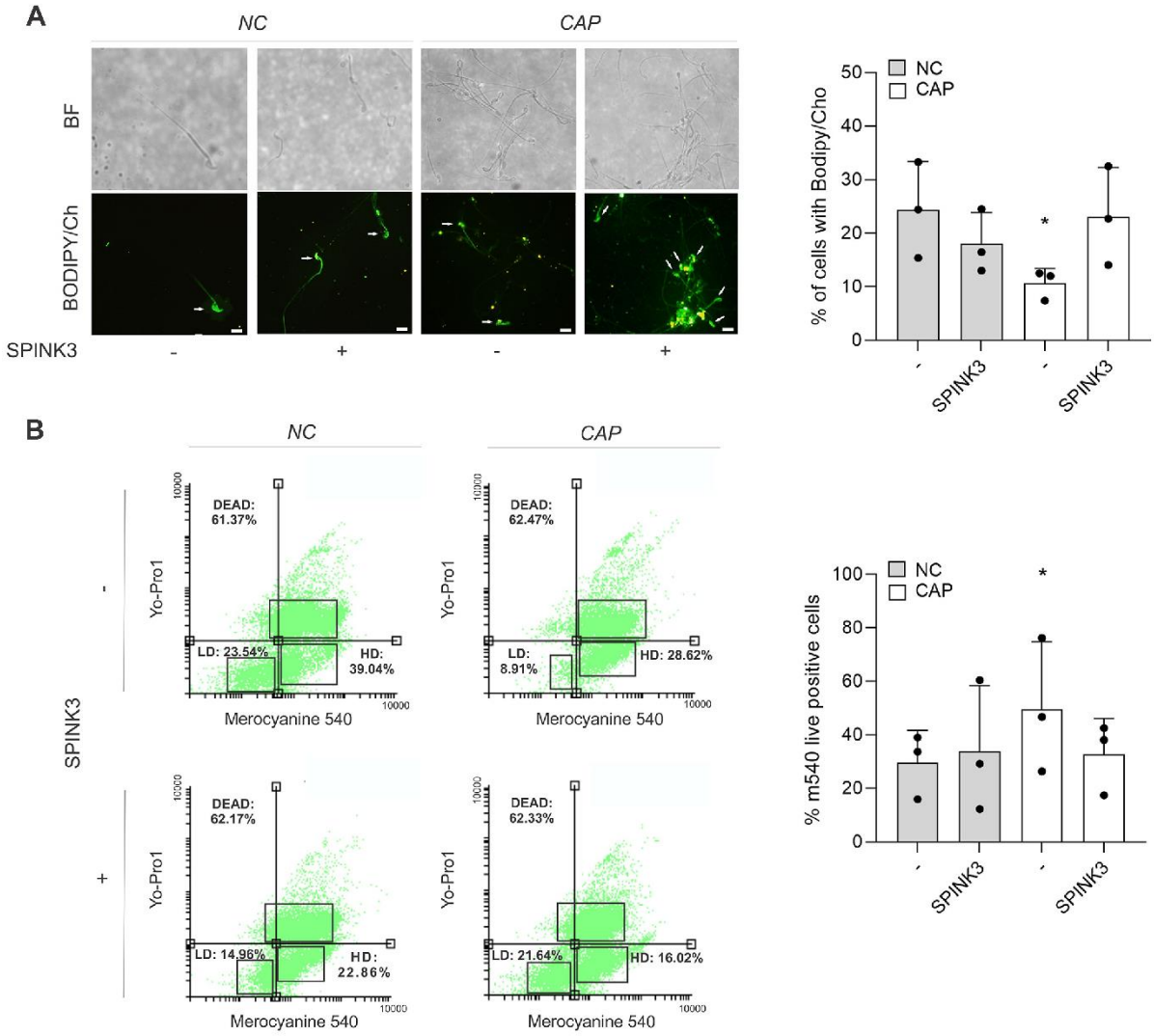

826
827 **Figure 4. SPINK3 blocks capacitation-associated cholesterol efflux and membrane**
828 **destabilization.** Mouse epididymal spermatozoa were loaded with Bodipy Cholesterol
829 (BODIPY/Ch) **(A)** or M540 and Yo-Pro1 **(B)** with or without SPINK3 (13 μM) and incubated
830 under capacitating (CAP) or non-capacitating (NC) conditions. n=3 LD: low disordered
831 membrane (Yo-Pro1$^-$/M540$^-$). HD: high disordered membrane (Yo-Pro1$^-$/M540$^+$). Percentage
832 of M540$^+$ cells is expressed relative to the total live cells (Yo-Pro1$^-$). (*) Significant differences
833 among treatments, p < 0.05. Scale bar: 10 μm.

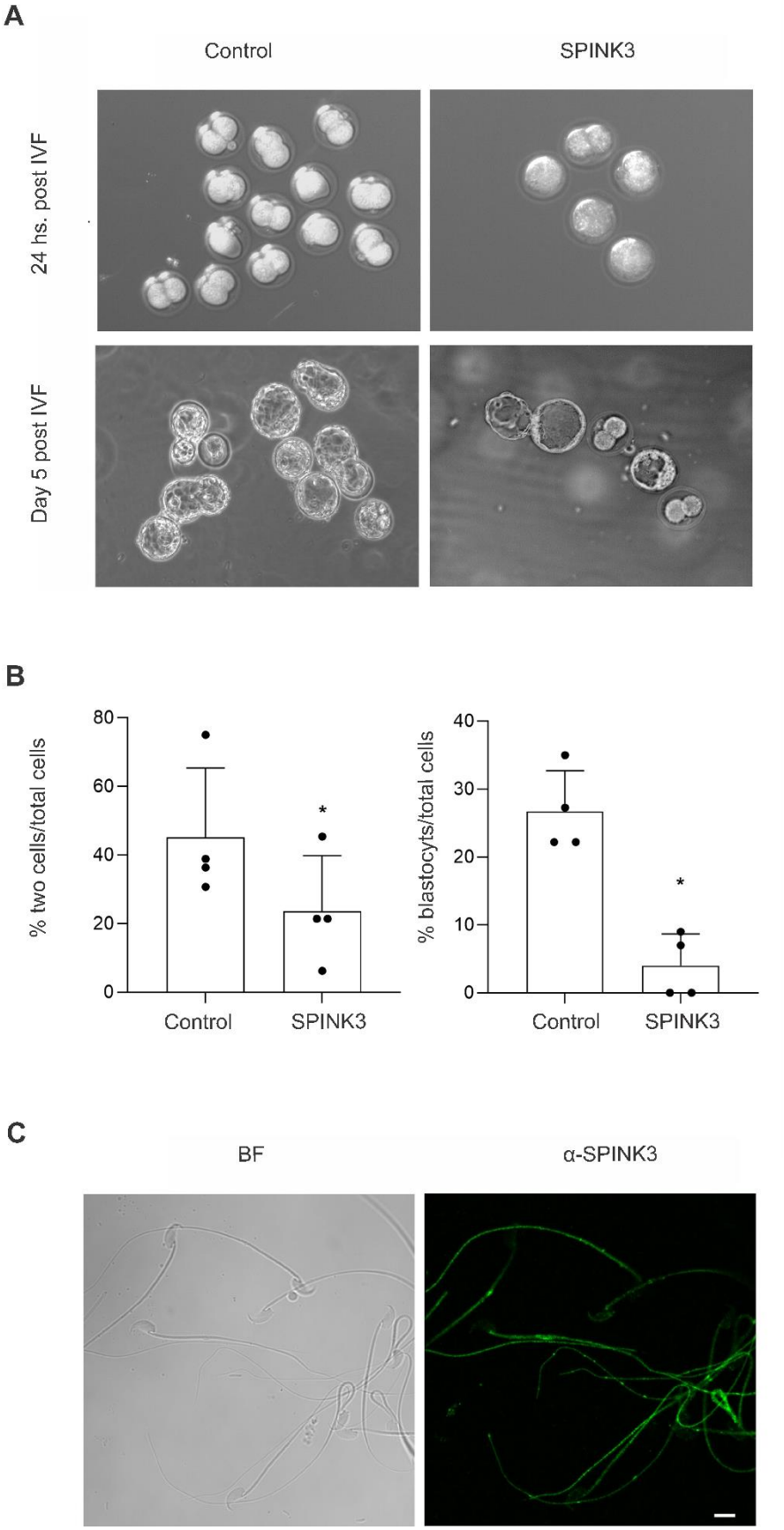

Figure 5. Effect of SPINK3 on *in vitro* fertilization. Mouse sperm were incubated in the absence or presence of rSPINK3 (13 μM) under capacitating conditions (CAP). After

837 capacitation, sperm (5 thousand total cells, 10 µl) were added to groups of COCs (5-6 COCs,
838 90 µl) obtained from superovulated females, (n=4). **A)** Representative images of two-cell
839 embryos and blastocysts obtained 24 hs. or 5 days post-IVF, respectively. **B)** Quantification
840 of two-cell embryos and blastocysts relative to the total oocytes (n=113). (*) Significant
841 differences compared to the control without SPINK3, $p < 0.05$. **C)** Sperm recovered after 4 hs.
842 of co-culture were incubated with α-SPINK3 antibodies to detect sperm-bound SPINK3 bound
843 to sperm by immunofluorescence. Scale bar: 10 µm.

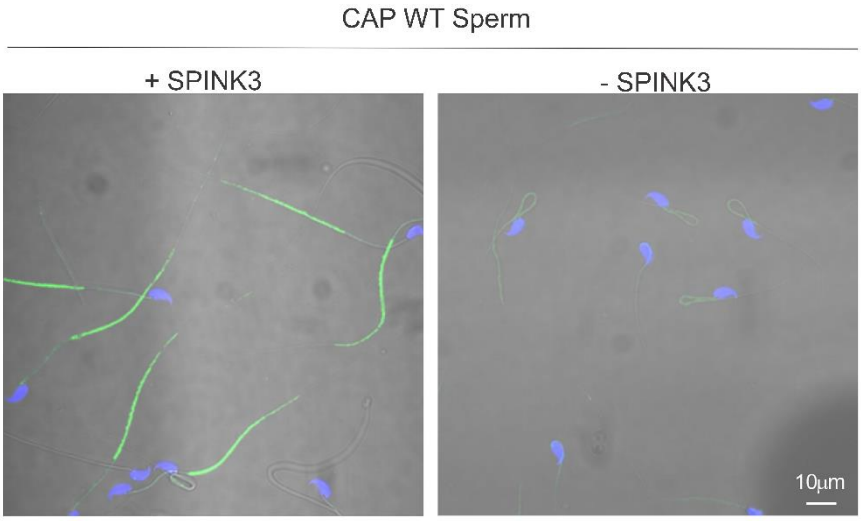

844
845 **Supplementary Figure 1.** Immunostaining was performed with anti-CATSPER1 antibody on
846 capacitated sperm that were previously incubated w/o SPINK3 for 30 min. Representative
847 images from three independent experiments are shown. Scale bar: 10 µm.

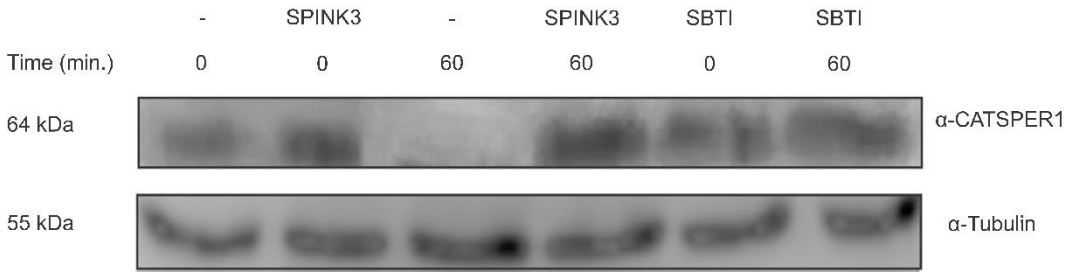

848
849 **Supplementary Figure 2.** *Effect of SPINK3 and SBTI on the proteolytic degradation of*
850 *CATSPER1 in vivo.* Mouse epididymal sperm (n=3) were incubated with or without SPINK3
851 (13 µM) or SBTI (1 µM) and exposed to CAP conditions. Cell lysis was performed on aliquots
852 of different treatments at 0 and 60 min. Proteins (0.5×10^6 cells/ml) were separated on a 10%
853 polyacrylamide gel and revealed by Western blot, using anti-CATSPER1 followed by anti-
854 Tubulin.

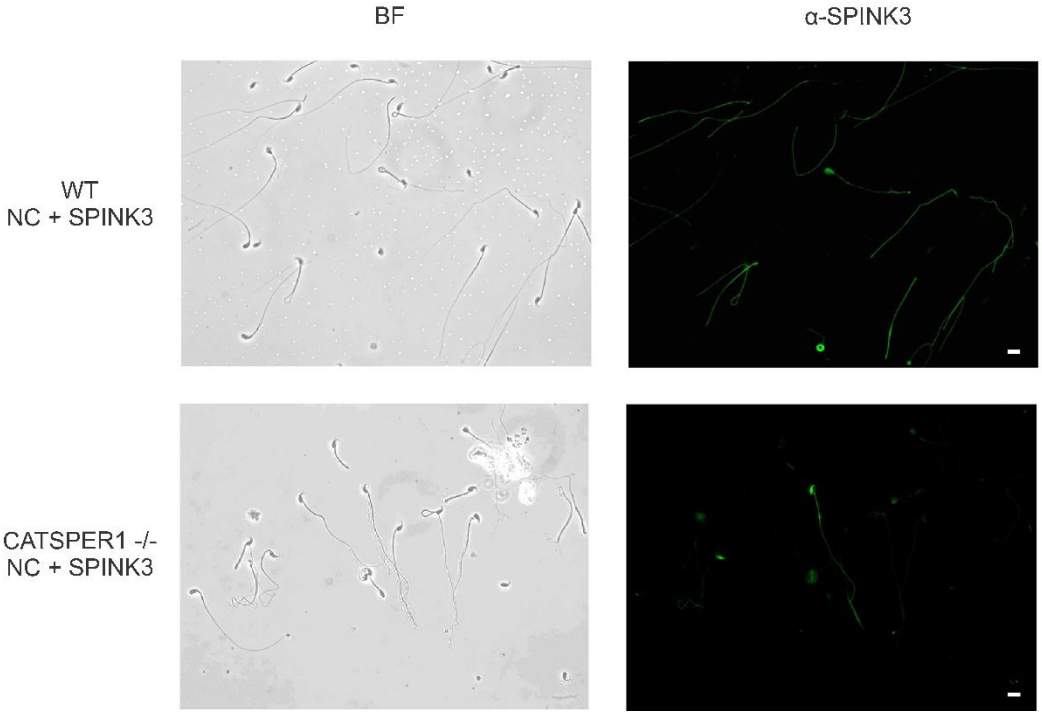

855
856 **Supplementary Figure 3.** *Immunodetection of recombinant SPINK3 incubated with*
857 *epididymal spermatozoa from wild type and Catsper1 KO mice.* Mouse epididymal NC
858 spermatozoa were incubated in the presence of SPINK3 (13 μM) and immunofluorescence
859 assays were performed using rabbit anti-SPINK3 (α-SPINK3) followed by anti-IgG-rabbit-
860 Alexa488 (green). (n=3) Scale bar: 10 μm. Images are representative of three independent
861 experiments. BF, bright field.

862

863 **Supplementary Movie 1.** *3D projection of SPINK3 and plasma membrane markers FM4-64*
864 *FX and CellBrite Fix on the sperm flagellum, related to Figure 2.* The video shows a rotating
865 view along the y-axis, providing a spatial visualization of SPINK3 (red) localization on the
866 plasma membrane of the sperm principal piece. The membrane is labeled with FM4-64 FX
867 (green) and CellBrite Fix (cyan), highlighting differences in staining intensity between the
868 midpiece and the principal piece. https://drive.google.com/drive/folders/1nl2lqlkbBCWcofPsq-
869 asTwwj_lwKv36C?usp=drive_link